Dynamics of Atmospheres and Oceans 93 (2021) 101186

Contents lists available at ScienceDirect

Dynamics of Atmospheres and Oceans

journal homepage: www.elsevier.com/locate/dynatmoce

Atmospheric driving mechanisms of extreme precipitation events in July of 2017 and 2018 in western Japan

Sridhara Nayak *, Tetsuya Takemi

Disaster Prevention Research Institute, Kyoto University, Kyoto, 6110011, Japan

ARTICLE INFO

Keywords:
Extreme precipitation event
Moisture advection
Moisture transport
Moisture flux convergence
Equivalent potential temperature

ABSTRACT

The occurrence of extreme precipitation events is now a serious concern in recent years in Japan. This study explores the atmospheric driving mechanisms of two extreme precipitation events occurred during 5–6 July 2017 and 5–8 July 2018 over western Japan. We identified that the atmospheric transport of large amounts of moisture and wind streams with wind speed of minimum 15 m s^{-1} from south of Japan towards north on the days before these torrential precipitation events are mainly responsible for the July 2017 and July 2018 floods over western Japan. However, the contributions from the moisture advections (both vertical and horizontal) to the atmospheric water budget plays key roles to intensify the precipitations during the said torrential events. We also find that the prominent moisture flux convergence and well-developed moist conditions mainly maintain these heavy precipitation events over the downpour affected area. Our overall analysis suggests that the atmospheric factors driving to all these two heavy precipitation events are qualitatively robust and vital to explain the mechanism of extreme precipitations.

1. Introduction

The increase in the intensity of extreme precipitation events over many regions across the globe is now a very serious concern (Intergovernmental Panel on Climate Change (IPCC), 2014). Empirical evidences (e.g., Yokoyama et al., 2017; Swain et al., 2018) as well as many modeling studies (e.g., Nayak and Dairaku, 2016; Nayak and Takemi, 2019) confirm such increase in the intensity of extreme precipitation events. As a consequence, lots of people worldwide are affected by excessive heavy rains each year. Therefore, the scientific understanding of the processes responsible for extreme precipitation events has become a challenging issue in recent years, although numerous studies have analyzed various extreme precipitation events over different regions (Ranalkar et al., 2016; Olsson et al., 2017; Kato et al., 2018; Panda and Sahu, 2019; Huang et al., 2019; Sahu et al., 2020).

During 5–6 July 2017 and 5–8 July 2018 two extremely heavy precipitation events occurred in western Japan. According to the observations by Japan Meteorological Agency, the daily precipitation amounts during these periods reached record breaking levels of over 500 mm d^{-1}. The event in 2017 spawned flooding and landslides in mountainous, limited regions concentrated in northern Kyushu Island, the westernmost major island of Japan. The 2018 event also caused flooding and landslides, but in more widespread regions in western Japan, and killed more than 200 people, which is the worst record among the meteorological disasters in the past 30 year or so. Understanding the mechanisms responsible to cause such extreme precipitations, therefore, is important not only from a

* Corresponding author.
E-mail address: nayak.sridhara.2n@kyoto-u.ac.jp (S. Nayak).

https://doi.org/10.1016/j.dynatmoce.2020.101186
Received 31 March 2020; Received in revised form 1 September 2020; Accepted 2 October 2020
Available online 25 December 2020

scientific point of view but also for a disaster prevention and mitigation perspective.

According to previous studies (Takemi, 2018; Kato et al., 2018; Tsuguti et al., 2019; Takemi and Unuma, 2019), such extremely torrential precipitation events in Japan are mainly associated with the Baiu frontal and typhoon activities and local convective systems. Besides this, topography, air mass, favorable synoptic situations and cold pools are also responsible to reproduce large precipitation amounts at a place (Ranalkar et al., 2016; Poulidis and Takemi, 2017; Takemi, 2018; Huang et al., 2019).

Although a flood event at a place depends on many factors as stated above, the torrential precipitation events that caused flooding depend on its dynamic and thermodynamic features such as wind speed and direction, moisture content, temperature etc. which characterize the maintenance of intense precipitation (Teixeira and Satyamurty, 2007; Milrad et al., 2015; Ranalkar et al., 2016; Nayak et al., 2018; Oueslati et al., 2019; Nayak and Takemi, 2020a, 2020b). Several studies have been carried out in order to understand the synoptic-scale pattern and convective systems of the torrential precipitation event during 5–6 July 2017 over northern Kyushu Island of Japan and 5–8 July 2018 over Shikoku Island of Japan (e.g. Takemi, 2018; Kato et al., 2018; Takemura et al., 2019; Tsuguti et al., 2019). Takemi (2018) reported that the July 2017 torrential event was produced due to the organization and maintenance of stationary connective systems over Kyushu Island and Tsuguti et al. (2019) highlighted that the July 2018 event was occurred due to the prolonged concentration of two very moist airstreams toward western Japan.

However, the atmospheric factors driving such extreme heavy precipitation events over western Japan have not been well explored from a mesoscale point of view. For example, the moisture advection both in the horizontal and vertical directions plays a very important role in understanding the development of convection and precipitation (Oueslati et al., 2019). Other atmospheric factors include moisture transport, stability, equivalent potential temperature, moisture flux convergences etc. and play important roles to storm initiation and subsequently cause excessive precipitation (Becker et al., 2009; Holman and Vavrus, 2012; Zhu and Hendon, 2015; Gao and Sun, 2016; Yamamoto, 2018; Oueslati et al., 2019). It is thus of much interest to understand the atmospheric forcing mechanism of different heavy precipitation events to explore their robust features. Our study intends to explore these atmospheric driving factors to understand their key roles in the organization and maintenance of the extreme precipitation events during 5–6 July 2017 and 5–8 July 2018 (hereafter J2017 and J2018) over western Japan in order to enhance the insights into the reason why the torrential precipitation occurred. For this purpose, we conduct regional-scale meteorological simulations with the Weather Research and Forecasting (WRF) model.

2. Data and methodology

As mentioned earlier, we have chosen two torrential precipitation cases (J2017 and J2018) over western Japan. The reason to

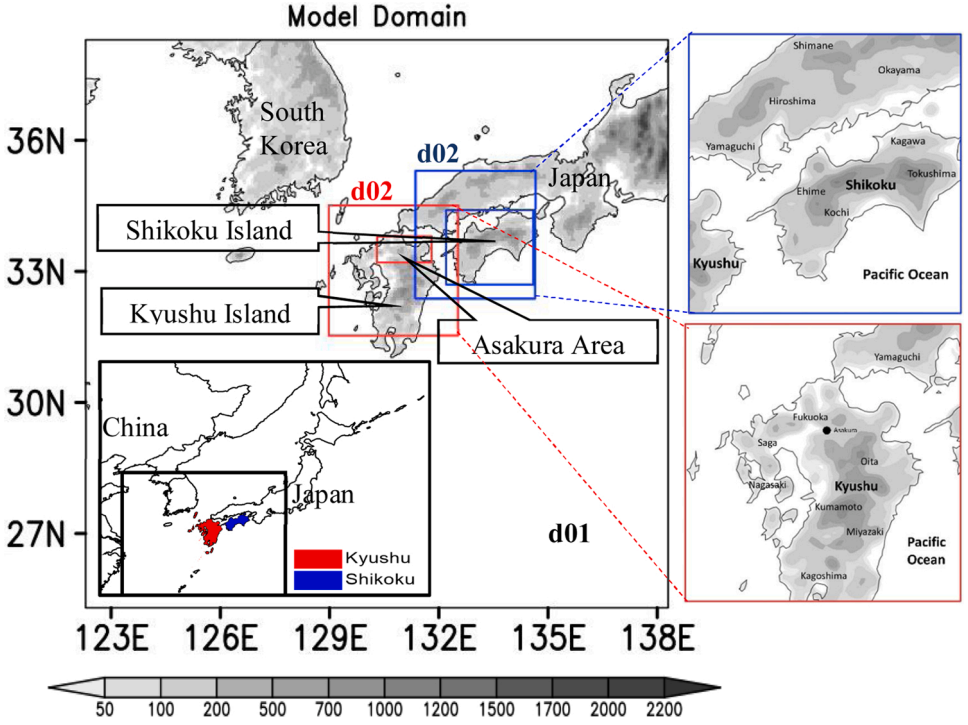

Fig. 1. Model domains with topography (unit: m). Gray shading indicates the outer domain (d01) with 5 km grid spacing. Red and blue colored inner domains (d02) correspond to the region with 1 km grid spacing for J2017 and J2018 event. The innermost box in each inner domain indicates the area over which the moisture budget components are computed. The inset map shows the location of the model domain with Kyushu and Shikoku Island of Japan. (For interpretation of the references to colour in this figure legend, the reader is referred to the web version of this article).

select these two precipitation events as our case studies was that these events brought record breaking levels of precipitation over 500 mm d^{-1} to western Japan and caused widespread flooding and landslides. Both precipitation events resulted huge economic losses with a large number of dead and missing people. A brief description of the two events is present here.

2.1. Overview of July 2017 heavy precipitation event

In early July 2017, extremely heavy rains caused by mesoscale lines of precipitation triggered deadly floods, landslides and house damages in Japan's southern island of Kyushu, and led to an advisory evacuation of nearly 500,000 people. A total of 42 people were dead or missing due to this torrential precipitation event. Because of the continuous heavy precipitation, northern Kyushu experienced heavy rain from July 5 to 6, 2017 and in some places the total precipitation surpassed the monthly average of July. A historic precipitation of 545.5 mm in 24 h in Asakura region of Fukuoka prefecture broke the observation records so far. The geographical location of this region is shown in Fig. 1.

2.2. Overview of July 2018 heavy precipitation event

From later June to early July 2018, downpours of heavy rains caused widespread havoc over western Japan due to the effects of Typhoon No. 7 (Prapiroon) and weather fronts, and led to an advisory evacuation of more than 8 million people. This event was one of the worst floods in Japan's history, causing over 200 dead and USD9.5 billion in economic losses. Due to this heavy precipitation event, some areas of Shikoku Island experienced record breaking precipitations over 1000 mm in 72 h (5–7 July 2018) which surpassed the monthly climatological normal for July since 1982. The location map of Shikoku Island is highlighted in Fig. 1.

2.3. Model setup and simulation methodology

We used the Advanced Research WRF model version 4.0 (Skamarock et al., 2008) configured in two-way interactive nested domains at spatial resolutions of 5 km (outer domain: d01) and 1 km (inner domain: d02) (Fig. 1). Both domains are encompassed with 56 vertical levels with 10 hPa model top. The model physics includes the rapid radiative transfer model scheme, the WRF single moment 6-class microphysics scheme, the Kain-Fritsch cumulus scheme (only for d01) and the Yonsei University planetary boundary layer scheme. To incorporate the synoptic-scale influences, the spectral nudging with 5 wave number in the x and y directions is used for d01.

We performed two numerical simulations (one simulation for J2017 and one simulation for J2018) with input from 1.25° resolution Japanese 55-year Reanalysis (JRA55) data (Kobayashi et al., 2015). For J2017 the model was initialized at 0000UTC 01 July 2017 and integrated until 0000UTC 07 July 2017, while for J2018 the model was initialized at 0000UTC 04 July 2018 and integrated until 0000UTC 09 July 2018. Results of the precipitation amounts over the model domains from each simulation are validated against the station observations from the Radar Automated Meteorological Data Acquisition System (Radar-AMeDAS) analyzed precipitation datasets. The Radar-AMeDAS observations are available over Japan and also known as the Radar/Rain gauge - Analyzed Precipitation product that provides the composite radar-derived precipitation maps calibrated with rain gauges.

2.4. Analysis method

To understand the maintenance of the extreme precipitations during J2017 and J2018 events, we analyzed the column integrated moisture flux convergence (MFC) to examine the areas where extreme precipitations occurred. The column integrated MFC is computed from the following equation.

$$MFC = -\frac{1}{g}\int_{1000}^{300} \nabla \cdot \left(q\vec{V}\right) dp \tag{1}$$

Where q is specific humidity, p is pressure, $\vec{V}$ is wind vector, g is the magnitude of the gravitational acceleration, ∇ is the horizontal gradient operator.

To understand the contribution from the moisture advections to the temporal evolution of precipitation, we decomposed and analyzed the moisture budget equation:

$$\frac{1}{g}\frac{\partial}{\partial t}\int_{1000}^{300} q\, dp = E - \frac{1}{g}\int_{1000}^{300} \omega \cdot \frac{\partial q}{\partial p} dp - \frac{1}{g}\int_{1000}^{300} \vec{V} \cdot \nabla q\, dp - P \tag{2}$$

Where q is specific humidity, p is pressure, ω is the pressure vertical velocity, $\vec{V}$ is wind vector, g is the magnitude of the gravitational acceleration, ∇ is the horizontal gradient operator, E is the surface evaporation, and P is the precipitation.

Symbolically,

$$S = E + V_{adv} + H_{adv} - P \tag{3}$$

Where S (left side on Eq. 2) is the time derivative of atmospheric q, often called storage, V_{adv} (the second term in right side on Eq. 2) is the vertical moisture advection, H_{adv} (the third term in right sight on Eq. 2) is the horizontal moisture advection.

To identify the origin of the moistures we then analyzed the moisture transports by integrating vertically the horizontal water vapor transport from the surface to the 300-hPa level with the following equation:

$$IVT = -\frac{1}{g}\int_{1000}^{300} q\vec{V}\,dp = \sqrt{\left(\frac{1}{g}\int_{1000}^{300} qu\,dp\right)^2 + \left(\frac{1}{g}\int_{1000}^{300} qv\,dp\right)^2} \tag{4}$$

where u is zonal wind, and v is meridional wind.

To further understand the atmospheric stability conditions and thereby the maintenance mechanisms of these two events, we analyzed the equivalent potential temperature (θ_e) from the following equation.

$$\theta_e = T_e\left(\frac{p_0}{p}\right)^{\frac{R_d}{c_p}} \approx \left(T + \frac{L_v}{c_p}r\right)\left(\frac{p_0}{p}\right)^{\frac{R_d}{c_p}} \tag{5}$$

Where T_e is the equivalent temperature, p_0 is the standard reference pressure (1000 hPa), p p is the pressure at the point, R_d is the specific gas constant for air (287 J kg^{-1} K^{-1}), c_p is the specific heat of dry air at constant pressure (1004 J kg^{-1} K^{-1}), T is the air temperature at pressure p p, L_v is the latent heat of evaporation, and r is the mixing ratio of water vapor.

3. Results and discussion

3.1. Precipitation distribution

First, the precipitation distributions of the two events simulated by the WRF simulations were compared with the Radar-AMeDAS observations. We examined the 12 -h accumulated precipitation on 5 July 2017 for J2017 and the 72 -h accumulated precipitation during 5–7 July 2018 for J2018 by considering the heavy precipitation active period for each event (Fig. 2). The results indicate that the total precipitation in the model simulations is underestimated over some regions compared to the Radar-AMeDAS observation in J2017, while it is overestimated compared to the Radar-AMeDAS observation in J2018. However, extremely heavy precipitations (> 500 mm) occurred around the Asakura area on 5 July 2017 and that of over 1000 mm in the Shikoku region during 5–7 July 2018 are

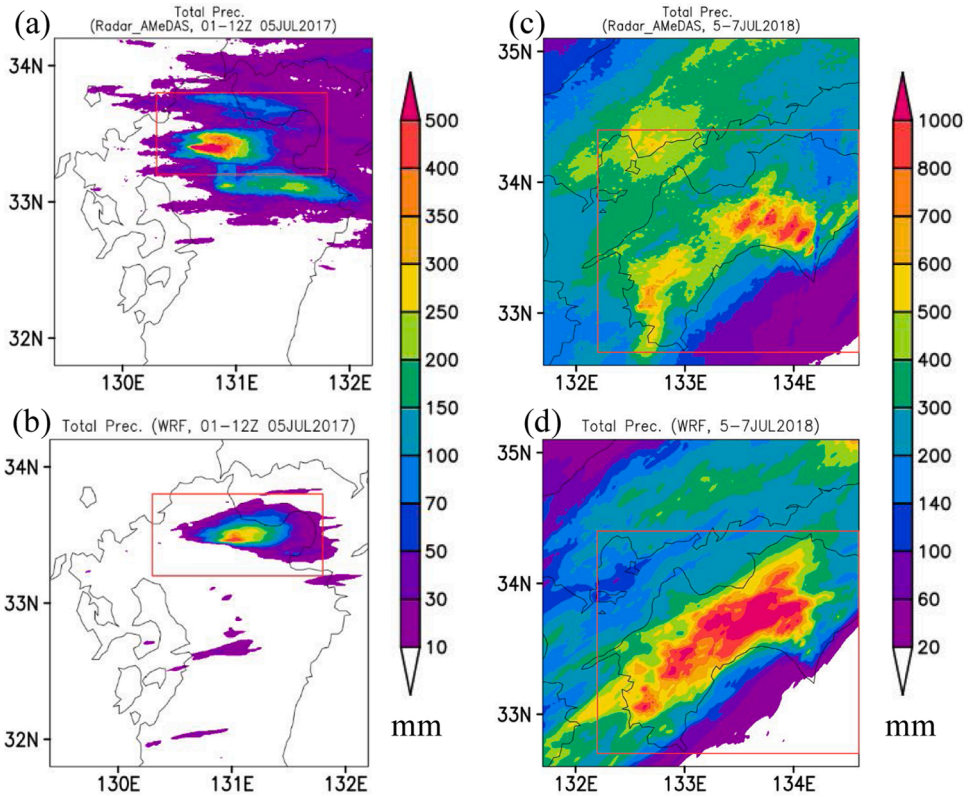

Fig. 2. 12 -hs (01-12UTC) accumulated precipitation on 5 July 2017 (a, b) and 72 -hs (00-23UTC) accumulated precipitation during 5-7 July 2018 (c, d). The upper panel corresponds to the precipitations from Radar-AMeDAS observation and lower panel corresponds to the precipitations from WRF simulation. The red box in each figure indicates the area over which the averaged and maximum precipitation are computed. (For interpretation of the references to colour in this figure legend, the reader is referred to the web version of this article).

well represented in the simulations.

The temporal variation of the hourly precipitation (area averaged, area maximum and frequency distribution) in the model simulations is compared with that of the Radar-AMeDAS observation in Fig. 3. For J2017, the simulation underestimates both the averaged and the maximum precipitation in the observation, although the shape of the temporal variations seems to be reproduced in the simulation. The pattern of simulated averaged and peak of the maximum precipitation for J2017 is comparable to that in the observation. For J2018, the observed averaged and maximum precipitation amount varies in the range of 1−10 mm and 20−170 mm, respectively, which are well captured in the simulations, although there are overestimations in the simulation for the maximum precipitation. The shape of frequency distributions of precipitation intensities (computed with all grid points) in both simulations of J2017 and J2018 agree reasonably well with that of in the observations, particularly for the stronger precipitations. The simulation of J2018 shows some stronger precipitations with intensities above 100 mm h^{-1} although their frequencies of occurrences are less.

Overall, the simulations were able to represent well the spatial distribution and temporal variation of precipitations in the J2017 and J2018 cases, in spite of some underestimations and overestimations of the simulated results compared with the observations. Based on this performance, we focus on the atmospheric forcing mechanisms of the J2017 and J2018 events.

3.2. Column integrated moisture flux convergence

To examine the areas where extreme precipitations occurred, we analyzed the column integrated MFC during J2017 and J2018 events from Eq. 1 and presented in Fig. 4. We find that the magnitude of MFC was maximum at around the Asakura area (130−132E &

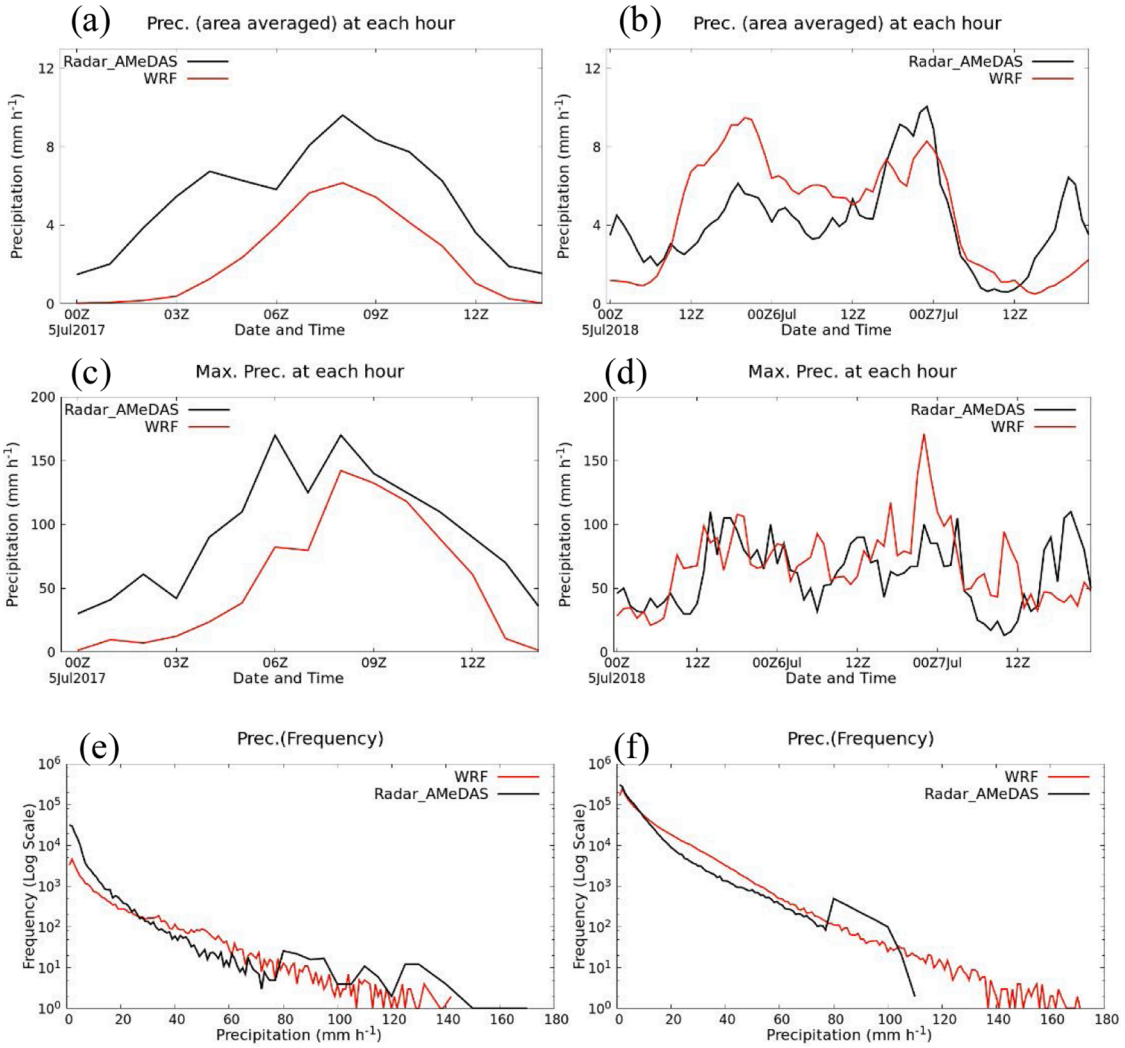

Fig. 3. Area averaged precipitation (a and b), area maximum precipitation (c and d) and frequency distributions of precipitations (e and f) over the red box region (see Fig. 2) at each hour during J2017 and J2018 event. (For interpretation of the references to colour in this figure legend, the reader is referred to the web version of this article).

33−34 N) on 5 July 2017 i.e. on the day of J2017 event (Fig. 4a–c). Maximum MFC was also noticed over Japanese land during 5–7 July 2018 (Fig. 4d–f). Closer investigation in Fig. 4 indicates that the MFC was prominent and continuous over the Asakura area during the J2017 event, while it was prolonged over Shikoku Island during J2018. Overall, the spatial structure of MFC shows that a dominant pattern of moisture source region for extreme precipitations during the J2017 and J2018 events result in bringing heavy precipitation to the Asakura area and the Shikoku region, because stronger MFC causes more convective instability to produce precipitation extremes (e.g. Becker et al., 2009; Holman and Vavrus, 2012).

3.3. Moisture advection

To understand the contribution from the moisture advections, we analyzed the decomposed terms of Eq. 3 at each hour (area averaged and area maximum) for the J2017 and J2018 events and illustrated in Fig. 5a and b. We find that the moisture advections (both vertical and horizontal) are maximum during the heaviest precipitation time of each event, indicating more moisture contributed towards the storage (S) to generate intense precipitation. We find small values of surface evaporation indicating less contribution to storage. For J2017 event, the area averaged V_{adv} and H_{adv} show maximum advections at 0800UTC 5 July 2017 before the heaviest precipitation occurs (Fig. 5a, c). Similar characteristics of V_{adv} and H_{adv} are noticed for J2018 event at 1700UTC 5 July 2018 (Fig. 5b, d). The contribution from V_{adv} to the storage shows moisture advection in the range of 1-1.5 mm h^{-1} during the maximum precipitation hours in the whole period of both J2017 and J2018 event, while that from H_{adv} shows moisture advection in the range of 8−9 mm h^{-1} during maximum precipitation hours. The analysis with the time at which maximum precipitation occurred indicates that minimum 20 mm h^{-1} of V_{adv} and at least 90 mm h^{-1} of H_{adv} contributed to the storage during both the events (Fig. 5e–h). These results suggest that the contributions from V_{adv} and H_{adv}, i.e. vertical and horizontal transport of moisture, moistened the troposphere to increase the water budget storage and made favorable for the development of convection to generate extreme precipitation events (e.g. Oueslati et al., 2019). For both the events (J2017 and J2018), we find similar characteristics of major contribution from H_{adv} to the time evolution of precipitation, indicating a robust mechanism of moisture advection in producing heavy precipitation during the torrential events over western Japan.

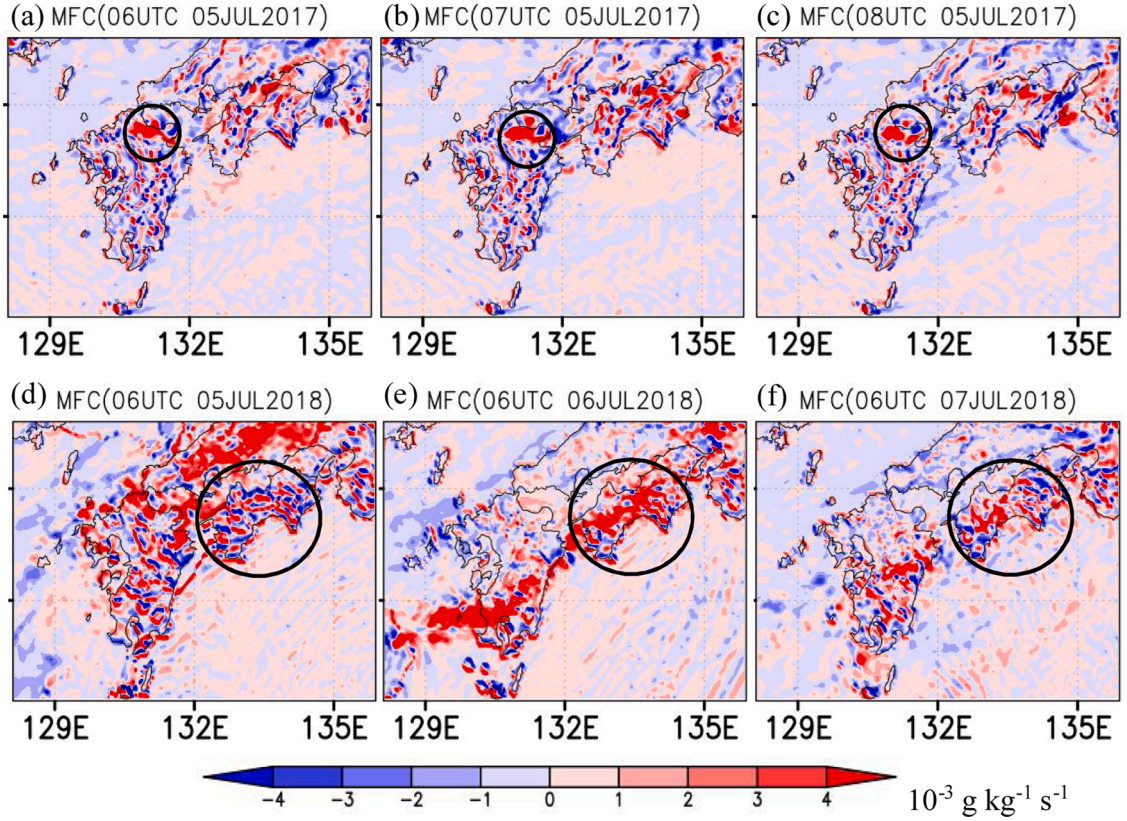

Fig. 4. Column integrated moisture flux convergence on the days of J2017 and J2018. (a–c) corresponds to the results for J2017 event; and (d–f) corresponds to results for J2018 event. The dates and times are indicated over each figure. Circles indicate the Asakura region for J2017 and Shikoku region for J2018 event.

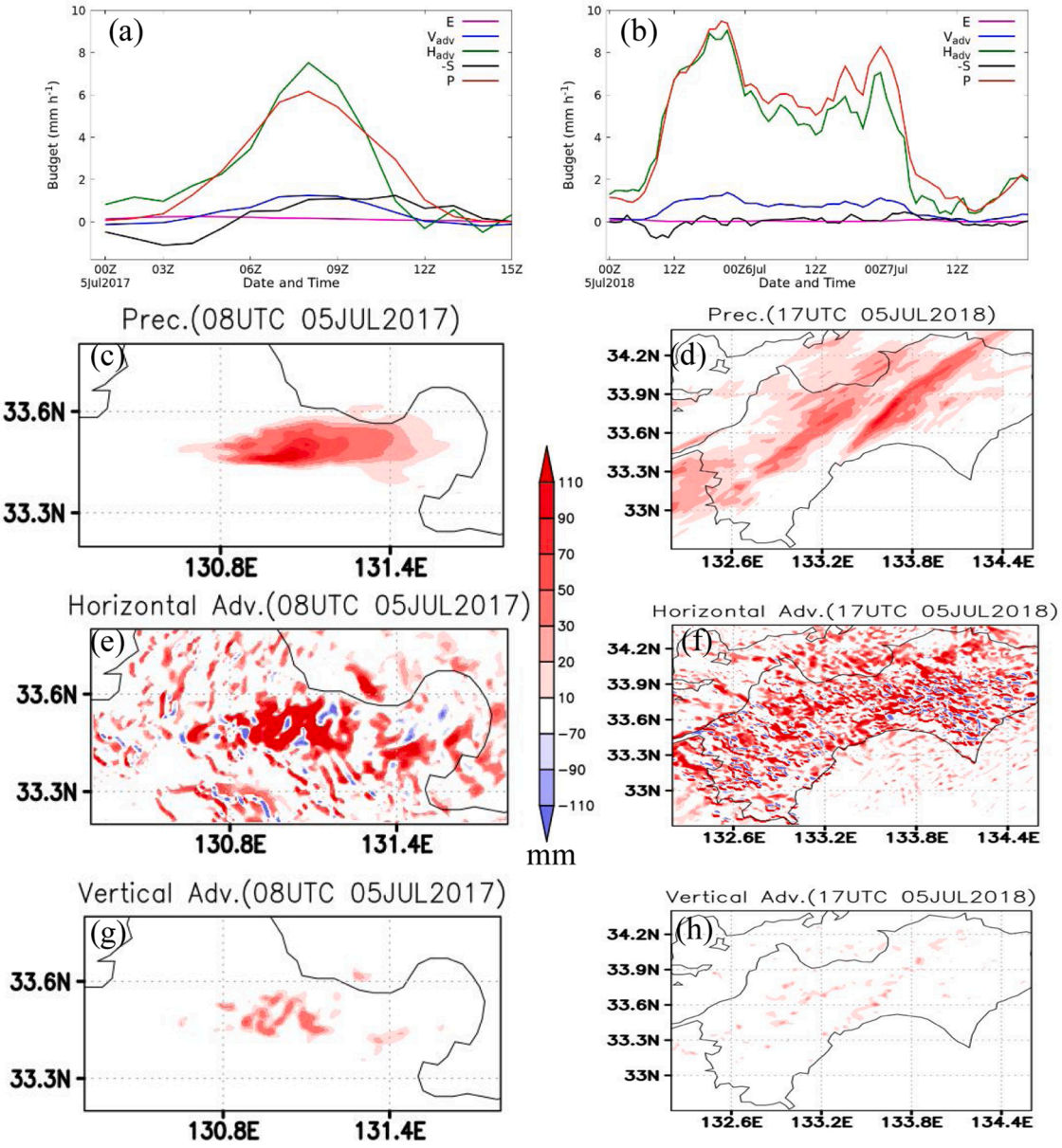

Fig. 5. (a, b) Area averaged moisture advections over the red box region (see Fig. 2) at each hour during J2017 and J2018 event. The Results in figures (a) and (b) corresponds to contributions from evaporation (magenta), vertical moisture advection (blue), horizontal moisture advection (green), and the storage (black). (c, d) Rainfall amount, (e, f) horizontal moisture advection and (g, h) vertical moisture advections during the maximum rainfall hour. (For interpretation of the references to colour in this figure legend, the reader is referred to the web version of this article).

3.4. Vertically integrated horizontal water vapor transport

To identify the origin of the moistures that was responsible for J2017 and J2018, we examined the vertically integrated horizontal water vapor transport (IVT). It is important to note that this water vapor must be available over certain areas prior to the extreme precipitation events. So we analyzed the moisture transports on the days before the torrential precipitation events occurred over the Kyushu and Shikoku regions from Eq.4. For J2017, we identified a large amount of moisture transport from the East China Sea region towards the Kyushu Island on 3 July 2017 (Fig. 6a–c). Over the East China Sea, the maximum IVT was located at around (126.5E, 28 N) at 0900UTC 3 July 2017 (Fig. 6a) which moved northward and located at around (127E, 29.5 N) at 1500UTC on the same day (Fig. 6b). This continued movement towards northern Kyushu and located at around the point 129E, 31 N at 2100UTC 3 July 2017. For J2018, a large amount of water vapor was transported northward from off the coast of the Shikoku Island during 4-6 July 2018 (Fig. 6d–f). Hirota et al. (2016) also highlighted that the intense moisture transport from the Indochina Peninsula to the Japanese islands was mainly responsible for the flash flood in Hiroshima on 19 August 2014. We also analyzed the IVT on 5 July 2017 at 0300UTC, 0600UTC

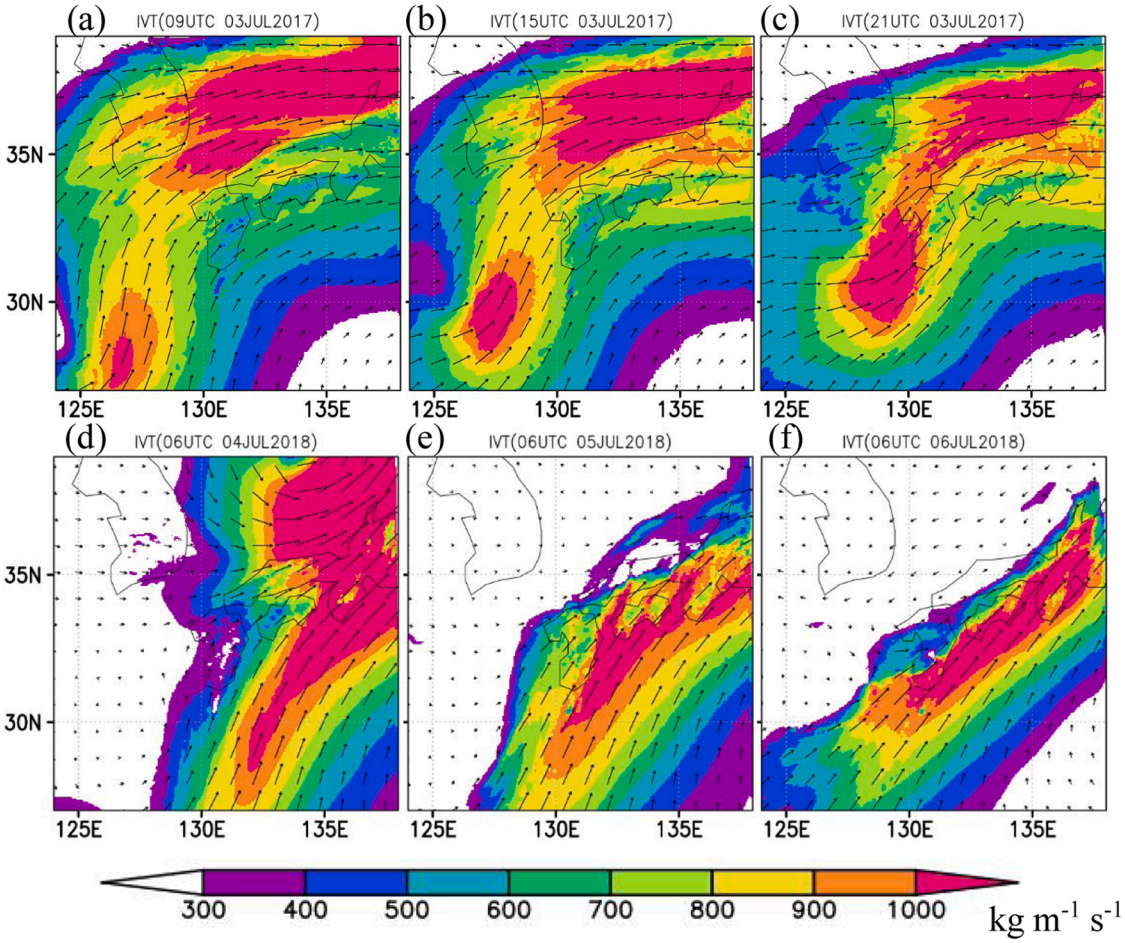

Fig. 6. IVT (color shading) at (a) 0900 UTC, (b) 1500 UTC, and (c) 2100 UTC on 3 July for J2017, and at (d) 0600 UTC 4 July, (e) 0600 UTC 5 July, and (f) 0600 UTC 6 July for J2018. Vectors (→) indicate 1000 kg m^{-1} s^{-1}.

and 0900UTC for the event J2017 and found the direction of IVT towards Kyushu Island with about 600 kg m^{-1} s^{-1} amount of moisture (figure not shown). For J2018, northward transport of a large amount of moisture (> 1000 kg m^{-1} s^{-1}) towards Shikoku Island was noticed on 5 July 2108 at 0300UTC and 0900UTC (figure not shown). The IVT on 5 July 2018 at 0600UTC is shown in Fig. 6e. These results indicate IVT plays an important role and show a robust feature leading to extremely heavy precipitations over northern Kyushu in 2017 and the Shikoku region in 2018.

Because the moisture transport is mainly controlled by the environmental steering flow, we analyzed the wind fields at the 500-hPa level on the days before the outbreaks of enhanced IVT (see Fig. 7). For J2017, the northeastward flows are noticed to the south of Japan at 0900UTC 3 July 2017 (Fig. 7a) which continued to move towards the north at 1500UTC 3 July 2017 (Fig. 7b) and finally moved towards north Kyushu with stronger winds at 2100UTC on the same day (Fig. 7c). Overall, we find a continuous northward flow greater than 15 m s^{-1} during 3 July 2017 towards Kyushu, similar to atmospheric moisture transports. In the J2018 case, flows towards Shikoku Island, with the magnitude greater than 15 m s^{-1}, are noticed on each day from 4 July 2018 until 6 July 2018 (Fig. 7d–f). This finding suggests that sufficiently strong southerly winds from the oceanic region to the south of Japan plays an important role to bring the moisture towards the Japanese Islands leading to the J2017 and J2018 events.

3.5. *Atmospheric stability*

To understand the atmospheric stability conditions during these two events, the equivalent potential temperature is examined at the 700-hPa level from Eq.5 and is shown in Fig. 8a–c. The θ_e for both the events are noticed to be a prolonged over towards Japanese land and lead to more convective activity to reproduce heavy precipitation events. The environmental conditions for the two events are examined by focusing on the atmospheric stability in terms of $d\theta_e/dz$ in the layers between 500-hPa and 850-hPa and is shown in Fig. 8e–h. Closer investigation shows much lower values (indicating highly unstable areas) over the Asakura region for the J2017 event on 5 July 2017 and that of over Shikoku Island for the J2018 event during 5–7 July 2018.

We also analyzed the developed moist conditions from relative humidity and air temperature at 500-hPa. This is shown in Fig. 9.

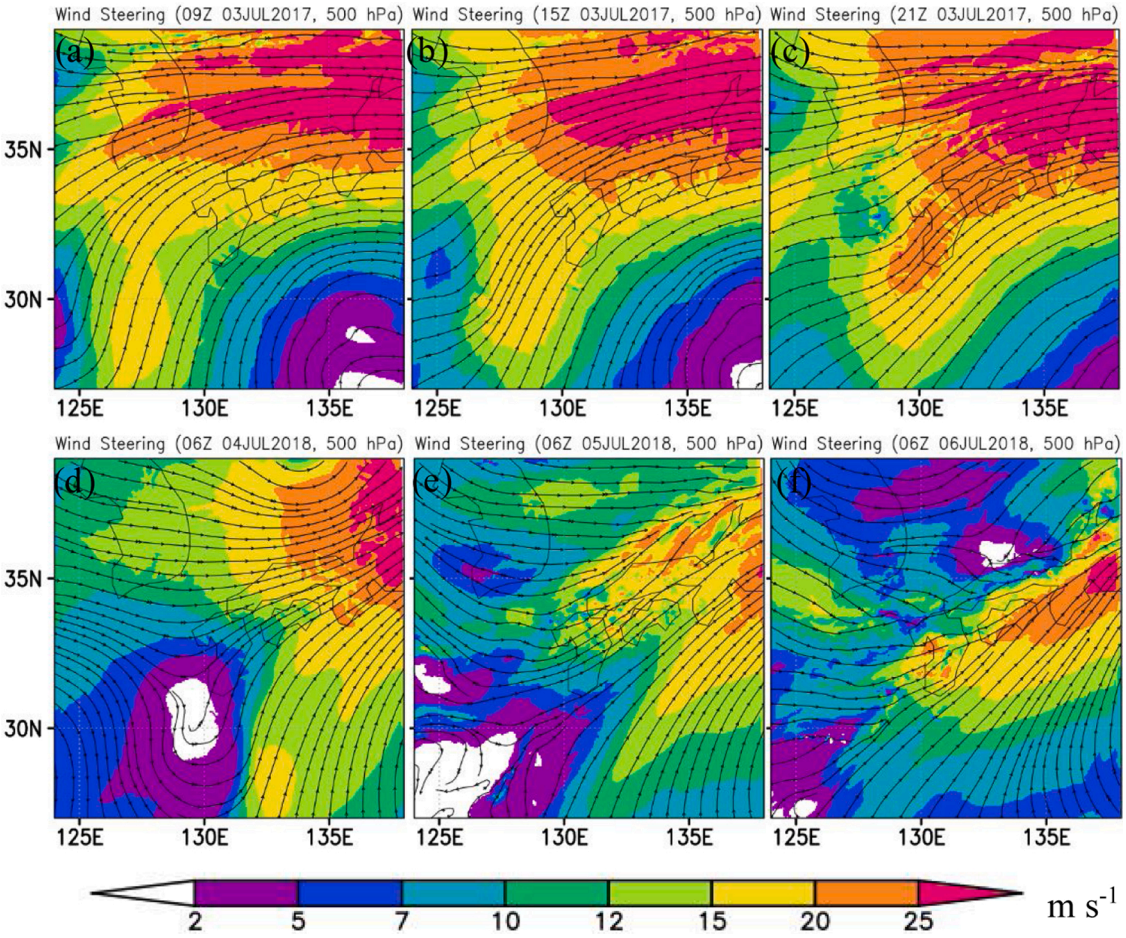

Fig. 7. The same as Fig. 5, but with streamlines and wind speed at the 500-hPa level.

We find high instability (Fig. 8e, h) together with colder conditions (Fig. 9a, d) and higher humid air inflow to the system (Fig. 9e, h) during these events. In moderate instability conditions (Fig. 8f, g), the 500-hPa level is warmer and still is very moist (Fig. 9b, c, f, g). All these conditions create most unstable atmospheric states and positively buoyant air to maintain the convectively unstable conditions (Kato, 2018). Previous studies (e.g., Kato, 2006) also highlighted similar atmospheric conditions for the heavy precipitation event on 29 June 1999 over northern Kyushu. We also analyzed the convective available potential energy (CAPE) on the days before J2017 and J2018 (Fig. 10) and noticed minimum 700 J kg^{-1} amount of CAPE over the Kyushu and Shikoku area. This indicates a sufficient amount of energy was available for the convection to cause the heavy precipitations during J2017 and J2018.

3.6. Comparison between J2017 and J2018 cases

In this section we compared the two events and their associated atmospheric driving mechanisms to explore their robust features. According to the Rada-AMeDAS observation, the J2017 event brought over 500 mm precipitation in a day while the J2018 event brought over 1000 mm in 72 h. The maximum hourly precipitation during the J2017 event in Asakura area was 170 mm while that of during J2018 event in Shikoku Island was about 100 mm. This implies that the J2017 event was short-lived with stronger precipitation intensity, while J2018 event was long-lived with relatively weaker precipitation intensity. However, both the events are maintained with favorable and robust environmental conditions to produce heavy precipitations. Stronger and mostly equal magnitudes of MFC are found over the Asakura area during the J2017 event and that of over Shikoku Island during the J2018 event. The characteristics of advection terms and their contribution to produce heavy precipitations are also found similar in both cases. A sufficiently strong southerly winds from the oceanic region to the south of Japan are noticed to bring the moisture towards the Japanese Islands leading to the heavy precipitations during J2017 and J2018 events. The overall results indicate that the atmospheric factors driving the J2017 and J2018 events are qualitatively similar, but quantitatively different. Higher CAPE is noticed on the days before both events, however, the CAPE in the case of J2017 was higher compared to that of the J2018 event (Fig. 10). Relative humidity and temperature at 500 hPa during the J2017 event was smaller than that of the J2018 event (Fig. 9). The $d\,\theta_e/dz$ and equivalent potential temperature during the J2017 event was also smaller compared to that of in the case of J2018 event (Fig. 2018). This implies that the atmosphere

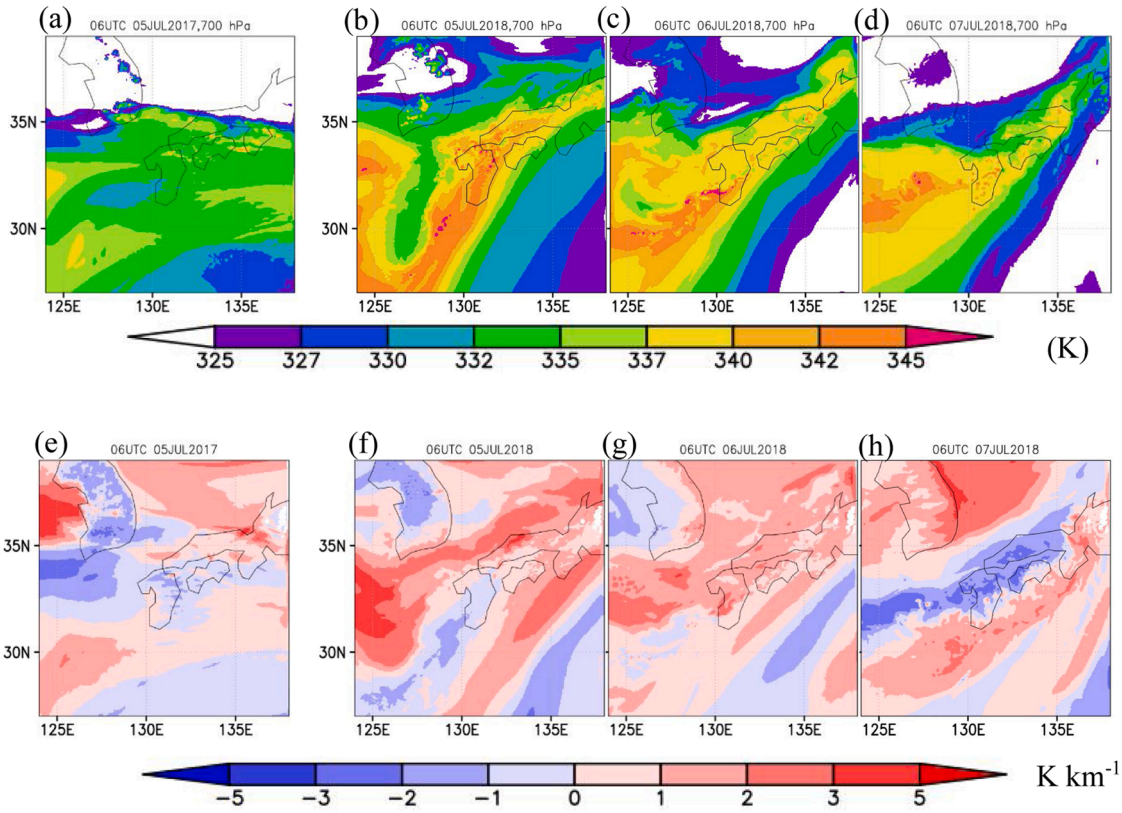

Fig. 8. Equivalent potential temperature at 700 hPa (1st row), $d\,\theta_e/dz$ between 500 hPa and 850 hPa (2nd row) on the days of J2017 and J2018. (a, e) corresponds to the results for J2017 event; and (b-d, f-h) corresponds to results for J2018 event. The dates and times are indicated over each figure.

during the J2017 event was more convectively unstable with stronger updrafts compared to that of during J2018 events, while the atmosphere during J2018 event was more humid than that of during J2017. It is noted that the J2018 case shows weak CAPE which should reproduce less amount of precipitation during J2018, but due to higher relative humidity and prolonged concentration of instability may develop the convection in a low CAPE environment (e.g., Takemi and Unuma, 2020).

As the occurrence of extreme precipitation events is increasing over western Japan (Koike, 2019), thus understanding the atmospheric systems for the relevance of extreme precipitation events is necessary to improve the forecasting of such events. Our results of moisture transport, stability, equivalent potential temperature, moisture flux convergences and water budget would help to understand the conditions underlying extreme precipitation events. It is worth to mention that our results are based on the WRF simulations which shows an underestimation of precipitation in J2017 and overestimation of precipitation in J2018. Thus more research is required to improve the simulation results for more robust understanding of the processes involved in extreme precipitation events. However, we believe that our study supplements to understand the atmospheric driving factors that are vital to explain the mechanism of extreme precipitation events and can be useful to comprehend similar precipitation events may occur in future over western Japan.

4. Conclusions and recommendations

In this study we analyzed the precipitation distributions of two extremely heavy precipitation events that occurred during 5–6 July 2017 and 5–8 July 2018 over Kyushu and Shikoku Islands of Japan, respectively by performing two simulations with the WRF model. We find that the model reproduced the extremely heavy precipitation amount ($>$ 500 mm d $^{-1}$) over Asakura area on 5 July 2017 and Shikoku region during 5–7 July 2018. The hourly precipitation patterns in the simulation also closely followed the Radar-AMeDAS observation. According to the previous studies (Takemi, 2018; Kato et al., 2018), the main cause of the July 2017 torrential precipitation event around Asakura was the result of back-building behavior of precipitation systems at a place over southern Japan for a long time. In general, this is a weather phenomenon when the deep convective clouds organize into clusters or lines over one location for several hours, known as stationary convective systems, to result in exceptionally a large amount of precipitation over a small area (Schumacher, 2009; Unuma and Takemi, 2016a, 2016b). The July 2018 heavy precipitation event was also caused due to the stationary convective systems although the Typhoon Prapiroon (T1807) had a large effect (Tsuguti et al., 2019). To understand more about the mechanism of these events (i.e. J2017 and J2018 events), we analyzed the atmospheric driving factors such as moisture advection, IVT, wind steering, atmospheric stability, equivalent potential temperature and column integrated MFC.

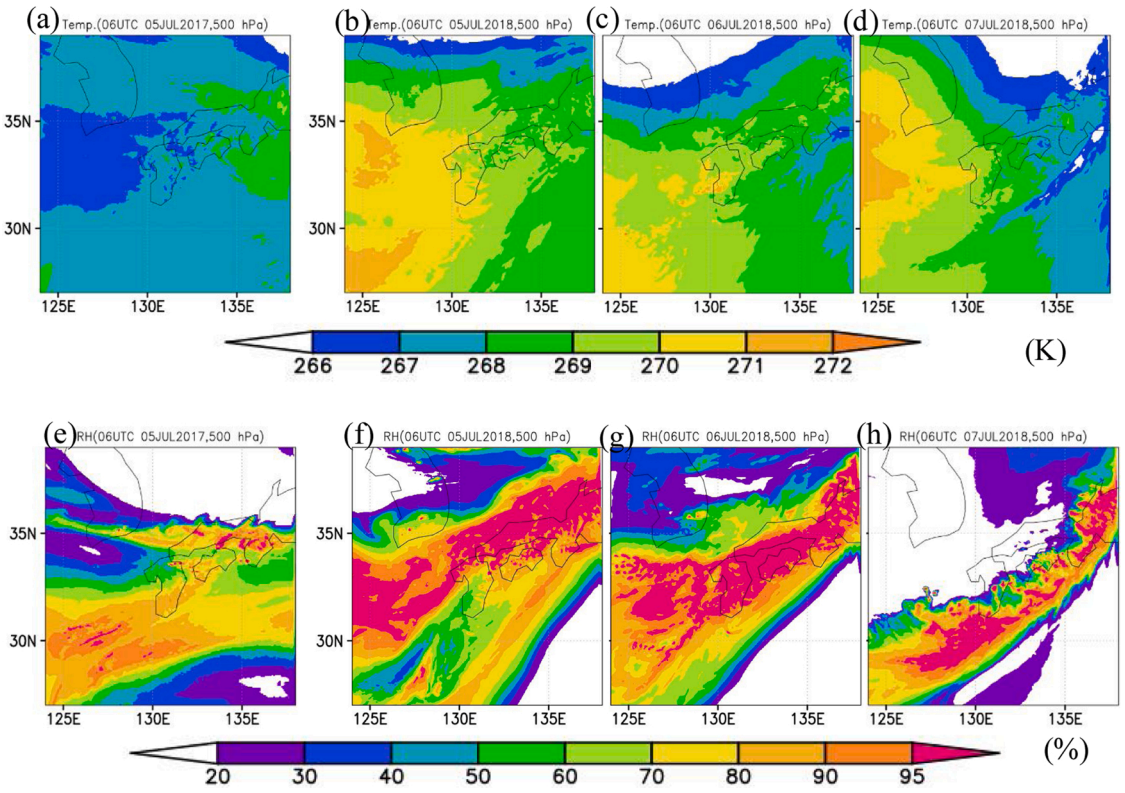

Fig. 9. Air temperature at 500 hPa (1st row) and relative humidity at 500 hPa (2nd row) on the days of J2017 and J2018. (a, e) corresponds to the results for J2017 event; and (b-d, f-h) corresponds to results for J2018 event. The dates and times are indicated over each figure.

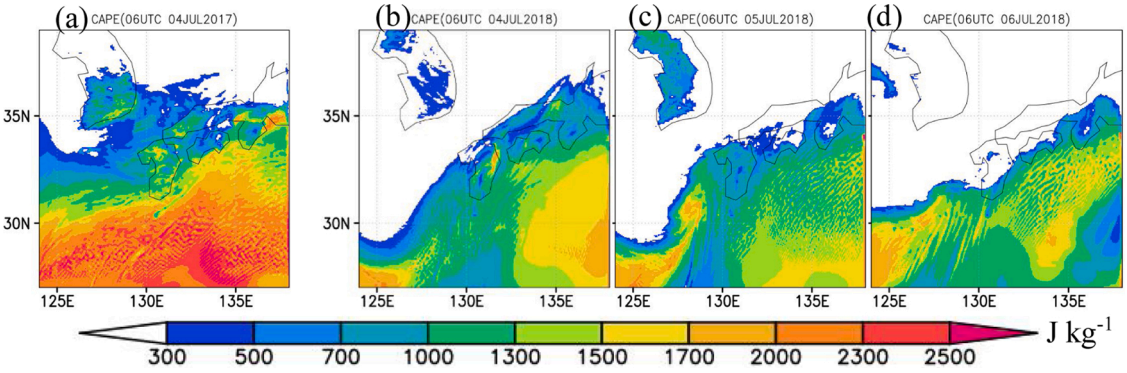

Fig. 10. CAPE on the days before of J2017 and J2018. (a) corresponds to the results for J2017 event; and (b–d) corresponds to results for J2018 event. The dates and times are indicated over each figure.

We identified that the contributions from vertical and horizontal moisture advections influence the atmospheric water budget and play a key role in intensifying the convective precipitations to produce large precipitation amounts during J2017 and J2018 events over north Kyushu and Shikoku region. In general, if more moisture is added to the storage then it may make favorable to cause heavier rains. Our results also show maximum contribution from V_{adv} and H_{adv} during the maximum precipitation hours during J2017 and J2018 events. We further identified that the atmospheric transport of a large amount of moisture from the south of Japan towards north on the days before J2017 and J2018 events is the main source for the extreme precipitation over north Kyushu and Shikoku region. Winds with the magnitude of at least 15 m s^{-1} were also noticed on the days before J2017 and J2018 events in the same directions as of IVT. Furthermore, higher values of equivalent potential temperature with humid airflow into the system and maximum MFC over Asakura area and Shikoku area during J2017 and J2018 events. These lead to unstable atmospheric conditions to cause precipitation extremes. Our overall analysis suggests that the atmospheric driving factors of both the events are qualitatively robust and are vital to explain the mechanism of extreme precipitation events.

Author statement

Sridhara Nayak proposed the topic, designed the study, analyzed the data and drafted the manuscript.
Tetsuya Takemi helped in the interpretation, editing and the construction of the manuscript.
All authors read and approved the final manuscript.

Declaration of Competing Interest

The authors declare that they have no known competing financial interests or personal relationships that could have appeared to influence the work reported in this paper.

Acknowledgments

This study is supported by the TOUGOU Program Grant Number JPMXD0717935498, funded by the Ministry of Education, Culture, Sports, Science, and Technology, Government of Japan. Japan Meteorological Agency (JMA) is acknowledged for providing the Radar-Automated Meteorological Data Acquisition System (Radar-AMeDAS) data.

References

Becker, E.J., Berbery, E.H., Higgins, R.W., 2009. Understanding the characteristics of daily precipitation over the United States using the North American Regional Reanalysis. J. Clim. 22 (23), 6268–6286.
Gao, Q., Sun, Y., 2016. Changes in water vapor transport during the Meiyu season after 2000 and their relationship with the Indian ocean SST and Pacific-Japan pattern. Dyn. Atmos. Ocean. 76, 141–153.
Hirota, N., Takayabu, Y.N., Kato, M., Arakane, S., 2016. Roles of an atmospheric river and a cutoff low in the extreme precipitation event in Hiroshima on 19 August 2014. Mon. Wea. Rev. 144 (3), 1145–1160.
Holman, K.D., Vavrus, S.J., 2012. Understanding simulated extreme precipitation events in Madison, Wisconsin, and the role of moisture flux convergence during the late twentieth and twenty-first centuries. J. Hydrometeorol. 13 (3), 877–894.
Huang, Y., Liu, Y., Liu, Y., Li, H., Knievel, J.C., 2019. Mechanisms for a record-breaking precipitation in the coastal metropolitan city of Guangzhou, China: observation analysis and nested very-large-eddy simulation with the WRF Model. J. Geophys. Res. Atmos. 124, 1370–1391.
Intergovernmental Panel on Climate Change (IPCC), 2014. Climate change 2014: synthesis report. In: Pachauri, R.K., Meyer, L.A. (Eds.), Contribution of Working Groups I, II and III to the Fifth Assessment Report of the Intergovernmental Panel on Climate Change. Geneva, Switzerland.
Kato, T., 2006. Structure of the band-shaped precipitation system inducing the heavy precipitation observed over northern Kyushu, Japan on 29 June 1999. J. Meteor. Soc. Japan Ser. II 84 (1), 129–153.
Kato, T., 2018. Representative height of the Low-Level Water Vapor Field for examining the initiation of moist convection leading to heavy precipitation in East Asia. J. Meteor. Soc. Japan Ser. II 96 (2), 69–83.
Kato, R., Shimose, K.I., Shimizu, S., 2018. Predictability of precipitation caused by linear precipitation systems during the July 2017 northern kyushu heavy precipitation event using a cloud-resolving numerical weather prediction model. Int. J. Disaster Resil. Built Environ. 13 (5), 846–859.
Kobayashi, S., Ota, Y., Harada, Y., Ebita, A., Moriya, M., Onoda, H., Onogi, K., Kamahori, H., Kobayashi, C., Endo, H., Miyaoka, K., Takahashi, K., 2015. The JRA-55 reanalysis: general specifications and basic characteristics. J. Meteor. Soc. Japan Ser. II. 93, 5–48.
Koike, T., 2019. 3. Mechanism, trends and DRR strategy of heavy Rain disaster in Western Japan. HELP Global Report on Water and Disasters, p. 28.
Milrad, S.M., Gyakum, J.R., Atallah, E.H., 2015. A meteorological analysis of the 2013 Alberta flood: antecedent large-scale flow pattern and synoptic–dynamic characteristics. Mon. Wea. Rev. 143 (7), 2817–2841.
Nayak, S., Dairaku, K., 2016. Future changes in extreme precipitation intensities associated with temperature under SRES A1B scenario. HRL. 10 (4), 139–144. https://doi.org/10.3178/hrl.10.139.
Nayak, S., Takemi, T., 2019. Dependence of extreme precipitable water events on temperature. Atmsfera 32 (2), 159–265. https://doi.org/10.20937/ATM.2019.32.02.06.
Nayak, S., Takemi, T., 2020a. Clausius-Clapeyron scaling of extremely heavy precipitations: case studies of the July 2017 and July 2018 heavy rainfall events over Japan. J. Meteorol. Soc. Jpn. 98 https://doi.org/10.2151/jmsj.2020-058.
Nayak, S., Takemi, T., 2020b. Typhoon-induced precipitation characterization over northern Japan: a case study for typhoons in 2016. Prog. Earth Planet. Sci. 7, 39. https://doi.org/10.1186/s40645-020-00347-x.
Nayak, S., Dairaku, K., Takayabu, I., Suzuki-Parker, A., Ishizaki, N.N., 2018. Extreme precipitation linked to temperature over Japan: current evaluation and projected changes with multi-model ensemble downscaling. Clim. Dyn. 51, 4385–4401. https://doi.org/10.1007/s00382-017-3866-8.
Olsson, J., Pers, B.C., Bengtsson, L., Pechlivanidis, I., Berg, P., Körnich, H., 2017. Distance-dependent depth-duration analysis in high-resolution hydro-meteorological ensemble forecasting: a case study in Malmö City. Sweden. Environ. Modell. Softw. 93, 381–397.
Oueslati, B., Yiou, P., Jézéquel, A., 2019. Revisiting the dynamic and thermodynamic processes driving the record-breaking January 2014 precipitation in the southern UK. Sci. Rep. 9 (1), 2859.
Panda, A., Sahu, N., 2019. Trend analysis of seasonal rainfall and temperature pattern in Kalahandi, Bolangir and Koraput districts of Odisha. India. Atmospheric Science Letters 20 (10), e932.
Poulidis, A.P., Takemi, T., 2017. A 1998–2013 climatology of Kyushu, Japan: seasonal variations of stability and precipitation. Int. J. Climatol. 37 (4), 1843–1858.
Ranalkar, M.R., Chaudhari, H.S., Hazra, A., Sawaisarje, G.K., Pokhrel, S., 2016. Dynamical features of incessant heavy precipitation event of June 2013 over Uttarakhand. India. Nat. Hazards 80 (3), 1579–1601.
Sahu, N., Panda, A., Nayak, S., Saini, A., Mishra, M., Sayama, T., Sahu, L., Duan, W., Avtar, R., Behera, S., 2020. Impact of indo-pacific climate variability on high streamflow events in Mahanadi River Basin. India. Water 12 (7), 1952.
Schumacher, R.S., 2009. Mechanisms for quasi-stationary behavior in simulated heavy-rain-producing convective systems. J. Atmos. Sci. 66 (6), 1543–1568.
Skamarock, W.C., Klemp, J.B., Dudhia, J., Gill, D.O., Barker, D.M., Duda, M.G., Huang, X., Wang, W., Powers, J.G., 2008. A description of the advanced research WRF version 3. Tech. Note 1–96.
Swain, M., Pattanayak, S., Mohanty, U.C., 2018. Characteristics of occurrence of heavy rainfall events over Odisha during summer monsoon season. Dyn. Atmos. Ocean. 82, 107–118.
Takemi, T., 2018. Importance of terrain representation in simulating a stationary convective system for the July 2017 Northern Kyushu Heavy Precipitation case. SOLA 14, 153–158. https://doi.org/10.2151/sola.2018-027.
Takemi, T., Unuma, T., 2019. Diagnosing environmental properties of the July 2018 Heavy Precipitation event in Japan. SOLA 15A, 60–65. https://doi.org/10.2151/sola.15A-011.
Takemi, T., Unuma, T., 2020. Environmental factors for the development of heavy precipitation in the eastern part of Japan during Typhoon Hagibis (2019). SOLA 16, 30–36. https://doi.org/10.2151/sola.2020-006.

Takemura, K., Wakamatsu, S., Togawa, H., Shimpo, A., Kobayashi, C., Maeda, S., Nakamura, H., 2019. Extreme moisture flux convergence over western Japan during the Heavy Rain Event of July 2018. SOLA 15A, 49–54.
Teixeira, M.S., Satyamurty, P., 2007. Dynamical and synoptic characteristics of heavy precipitation episodes in southern Brazil. Mon. Wea. Rev. 135 (2), 598–617.
Tsuguti, H., Seino, N., Kawase, H., Imada, Y., Nakaegawa, T., Takayabu, I., 2019. Meteorological overview and mesoscale characteristics of the Heavy Rain Event of July 2018 in Japan. Landslides 16 (2), 363–371.
Unuma, T., Takemi, T., 2016a. A role of environmental shear on the organization mode of quasi-stationary convective clusters during the warm season in Japan. SOLA 12, 111–115.
Unuma, T., Takemi, T., 2016b. Characteristics and environmental conditions of quasi-stationary convective clusters during the warm season in Japan. Q. J. R. Meteorol. Soc. 142 (696), 1232–1249.
Yamamoto, M., 2018. Migration of contact binary cyclones and atmospheric river: case of explosive extratropical cyclones in East Asia on December 16, 2014. Dyn. Atmos. Ocean. 83, 17–40.
Yokoyama, C., Takayabu, Y.N., Horinouchi, T., 2017. Precipitation characteristics over East Asia in early summer: effects of the subtropical jet and lower-tropospheric convective instability. J. Clim. 30 (20), 8127–8147.
Zhu, H., Hendon, H., 2015. Role of large-scale moisture advection for simulation of the MJO with increased entrainment. Q. J. R. Meteorol. Soc. 141 (691), 2127–2136.